

Newton Raphson Load Flow Analysis For IEEE-14 Bus Power Transmission Network

Victor Etop Sunday¹

Department of Electrical/Electronic Engineering,
University of Uyo, Akwa Ibom, Nigeria

Nseobong Okpura²

Department of Electrical/Electronic Engineering,
University of Uyo, Akwa Ibom, Nigeria

Kufre Michael Udofia³

Department of Electrical /Electronic Engineering,
University of Uyo, Akwa Ibom State, Nigeria

Abstract— In this work, Newton Raphson load flow analysis for IEEE-14 bus power transmission network is presented. The core objective of the load flow analysis was to validate system performance across six principal electrical dimensions: per-bus voltage profile, real and reactive power mismatch, transmission line power flow and associated losses, slack bus performance over time, voltage stability margins, and temporal variations of network behavior. The results show that the highest active power transfer is observed along the line 1–5 (229.10 MW), which corresponds to one of the key transmission corridors linking the main generation centers with significant load areas. Similarly, the line 2–4 carries a substantial active load of 140.42 MW, indicating its strategic role in supporting the power transfer towards downstream buses. Also, the active power injection by the slack bus fluctuates significantly across the simulation horizon, with observed values ranging from approximately 15.59 MW at the lower end (e.g., 19:00 hours on December 31st) to peaks exceeding 85 MW (e.g., 01:00 hours on January 1st). This variation reflects the diurnal and seasonal changes in load demand patterns, as well as the contribution of other generation units within the system. Similarly, reactive power injection exhibits substantial variability, with values ranging from about 6.48 MVAR to nearly 71.55 MVAR over the year. Furthermore, the results reveals that the voltage magnitudes remained within the acceptable regulatory bounds of 0.94 to 1.06 per unit. This compliance across all 14 buses is a critical indicator of proper reactive

power balance, controlled network loading, and sufficient voltage support mechanisms within the modeled network.

Keywords— *Power Transmission Network, Load Flow Analysis, IEEE-14 Bus System, Newton Raphson Method, Single-Line Topology Model*

1. Introduction

The IEEE 14-Bus transmission network is a widely recognized benchmark for power system analysis and optimization studies [1,2,3]. Generally, to establish a robust and accurate reference point for assessing the performance of power transmission network optimization models, load flow analysis need to be conducted [4,5]. Equally, load flow analysis is required after the power network optimization models are implemented [6,7,8]. The results of the load flow analysis before and after the power network optimization models are implement are used to assess the effectiveness of the optimization models in stabilizing the power network voltage profile and in minimizing the active and reactive power losses [9,10,11].

In practices, there are several methods of conducting load flow analysis [12,13,14]. In this work, the load flow analysis is conducted using the Newton-Raphson (NR) method [15,16,17]. The NR method, widely acknowledged for its rapid convergence and numerical stability, was selected due to its superior capability in handling large, sparse, and nonlinear algebraic equations typically encountered in power systems analysis. The Newton-Raphson method operates by iteratively solving the nonlinear power flow equations that relate bus voltages, power injections, and network admittance [25]. Notably, the core objective of the load flow analysis in this work is

to validate system performance across six principal electrical dimensions: per-bus voltage profile, real and reactive power mismatch, transmission line power flow and associated losses, slack bus performance over time, voltage stability margins, and temporal variations of network behavior.

2. Methodology

2.1 The IEEE-14 bus power transmission network model and parameters used for the analysis

This study seeks to conduct load flow analysis on the IEEE 14-Bus transmission network. The IEEE 14-bus

power transmission network model is presented in Figure 1. The transmission line parameters and transformer settings for IEEE 14-bus transmission network are presented in Table 1. The IEEE 14-bus transmission network modeling process, executed within MATLAB Simulink (R2023a), involved detailed parameterization of the electrical infrastructure, encompassing generator units, transmission line impedances, transformer tap settings, reactive power compensators, and static and dynamic load profiles, reflecting the physical and operational realities of a mid-scale electric grid.

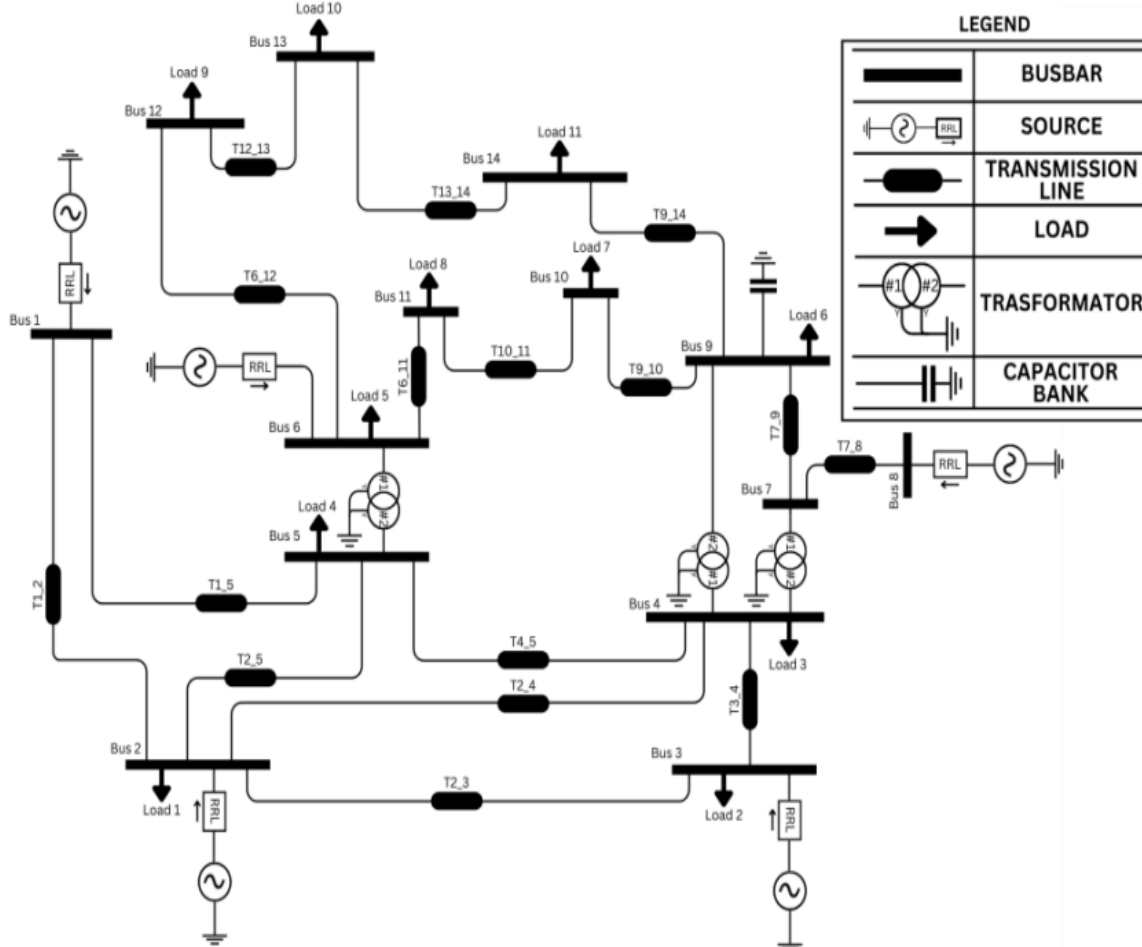


Figure 1 The IEEE 14-bus power transmission network single-line topology model [19]

Table 1: Transmission Line Parameters and Transformer Settings for IEEE 14-Bus power transmission network

From-To	R (p.u.)	X (p.u.)	Z (p.u.)	Z (Ω)	Length (km)	B/2 (p.u.)	Tap Ratio
1-2	0.01938	0.05917	0.06226	11.86	29.4	0.01320	1.000
1-5	0.05403	0.22304	0.22946	43.72	108.5	0.01230	1.000
2-3	0.04699	0.19797	0.20351	38.79	96.3	0.01095	1.000
2-4	0.05811	0.17632	0.18569	35.36	87.8	0.00850	1.000
2-5	0.05695	0.17388	0.18293	34.85	86.5	0.00865	1.000
3-4	0.06701	0.17103	0.18461	35.17	87.3	0.00320	1.000
4-5	0.01335	0.04211	0.04417	8.41	20.9	0.00000	1.000
4-7	0.00000	0.20912	0.20912	39.83	98.9	0.00000	0.978
4-9	0.00000	0.55618	0.55618	105.92	262.8	0.00000	0.969
5-6	0.00000	0.25202	0.25202	47.99	119.1	0.00000	0.932
6-11	0.09498	0.19890	0.22023	41.96	104.1	0.00000	1.000
6-12	0.12291	0.25581	0.28302	53.90	133.7	0.00000	1.000
6-13	0.06615	0.13027	0.14630	27.88	69.2	0.00000	1.000
7-8	0.00000	0.17615	0.17615	33.54	83.2	0.00000	1.000
7-9	0.00000	0.11001	0.11001	20.97	52.0	0.00000	1.000
9-10	0.03181	0.08450	0.09028	17.20	42.7	0.00000	1.000
9-14	0.12711	0.27038	0.29920	56.98	141.4	0.00000	1.000
10-11	0.08205	0.19207	0.20878	39.75	98.6	0.00000	1.000
12-13	0.22092	0.19988	0.29852	56.84	141.0	0.00000	1.000
13-14	0.17093	0.34802	0.38680	73.71	183.0	0.00000	1.000

2.2 The Newton Raphson Load Flow Technique for Baseline Modelling

In this work, the load flow analysis is conducted using the Newton-Raphson (NR) method. The Newton-Raphson method operates by iteratively solving the nonlinear power flow equations that relate bus voltages, power injections, and network admittance. For each bus i in a power system with N buses, the real and reactive power mismatches are calculated using:

$$\Delta P_i = P_i^{scheduled} - P_i^{calculated}, \quad \Delta Q_i = Q_i^{scheduled} - Q_i^{calculated} \quad (1)$$

Where, $P_i^{scheduled}$ is the scheduled active power at bus i , $P_i^{calculated}$ is the calculated active power at bus i , $Q_i^{scheduled}$ is the scheduled reactive power at bus i , $Q_i^{calculated}$ is the calculated reactive power at bus i .

These mismatches are functions of the voltage magnitudes and phase angles at all buses. The iterative process updates these state variables using the Jacobian matrix J of partial derivatives, yielding the following update formulation:

$$\begin{bmatrix} \Delta \theta \\ \Delta |V| \end{bmatrix} = J^{-1} \begin{bmatrix} \Delta P \\ \Delta Q \end{bmatrix} \quad (2)$$

Where, $\Delta \theta$ and $\Delta |V|$ are correction to bus voltage angles and magnitudes, J is the Jacobian matrix, ΔP and ΔQ are active and reactive power mismatches.

The iteration continues until a maximum mismatch $\max(|\Delta P|, |\Delta Q|)$ falls below a predefined convergence tolerance, set at 10^{-4} . In this study, the IEEE 14-bus test network was modeled using per-unit parameters, with all generation, load, and line data transformed accordingly.

The NR method was implemented using the polar form, where voltages are expressed as magnitude and angle, and power mismatches are resolved through successive linearization of the nonlinear power flow equations. Three types of buses were defined as per standard convention:

- i. Slack Bus (Bus 1): Maintains system voltage magnitude and phase reference.
- ii. PV Buses: Generator buses with specified real power and voltage magnitude.
- iii. PQ Buses: Load buses with specified active and reactive power demands.

For each iteration, the real and reactive power at each bus were computed using:

$$P_i = \sum_{j=1}^N |V_i| |V_j| (G_{ij} \cos \theta_{ij} + B_{ij} \sin \theta_{ij}) \quad (3)$$

$$Q_i = \sum_{j=1}^N |V_i| |V_j| (G_{ij} \sin \theta_{ij} - B_{ij} \cos \theta_{ij}) \quad (4)$$

Where, G_{ij} and B_{ij} are the real and imaginary parts of the admittance matrix, $\theta_{ij} = \theta_i - \theta_j$ is the phase angle difference between buses i and j .

The computed bus powers were compared against the scheduled values to determine mismatch vectors. The Jacobian matrix was updated accordingly in each iteration to determine the required corrections. This process was automated via a customized MATLAB-based implementation, ensuring consistent performance and reproducibility. The NR method's numerical precision enabled the isolation of power mismatch patterns at each node and highlighted key areas of energy loss. The

flowchart for the Newton-Raphson load flow analysis is presented in Figure 2.

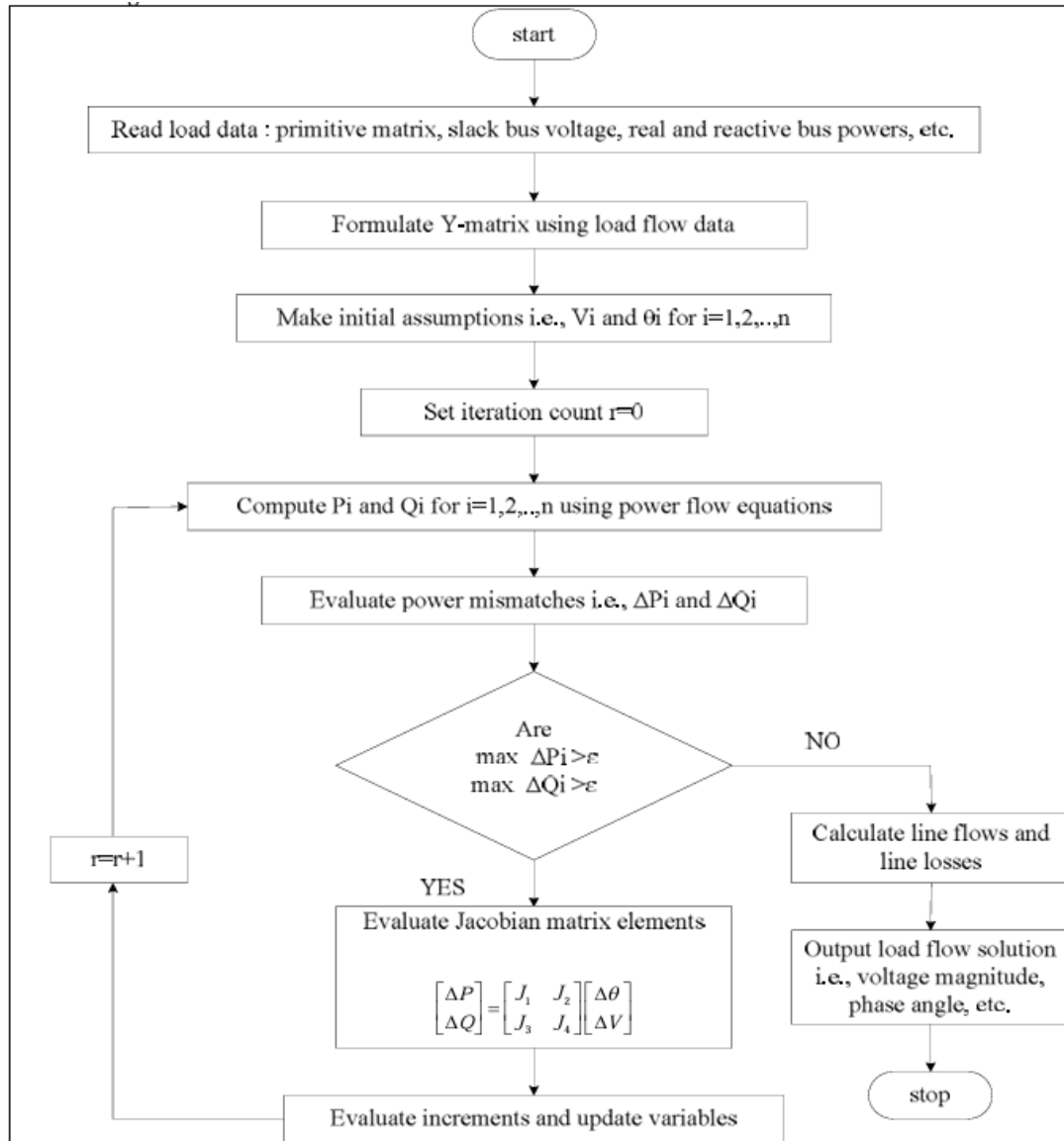


Figure 2 The flowchart of the Newton Raphson Load Flow Analysis [20]

The IEEE 14-bus single-line topology, previously modelled and parameterized using standard generator capacities, transmission line impedances, and transformer tap settings, served as the simulation environment. The core objective of the load flow analysis was to validate system performance across six principal electrical dimensions:

- i. Per-bus voltage profile,
- ii. Real and reactive power mismatch,
- iii. Transmission line power flow and associated losses,
- iv. Slack bus performance over time,
- v. Voltage stability margins, and
- vi. Temporal variations of network behavior.

To achieve this, a customized Python-based simulation pipeline was developed. The preprocessed dataset was parsed to evaluate each electrical dimension per timestamp and per bus using analytical approximations of power flow

quantities and mismatch formulations. While Newton-Raphson power flow algorithm (Figure 2) was employed at this stage, approximated load flow quantities were inferred from scheduled (dataset-defined) and computed values using standard deviation-based perturbations to simulate calculation uncertainties, hence replicating realistic mismatch conditions.

3. Results and discussion

All results from this analysis were visualized through both graphical (plots and heatmaps) and tabular formats as. Voltage profiles, loss distributions, slack bus behaviour, and stability indices were each captured for selected timestamps (e.g., peak and off-peak periods), providing insights into the natural operating performance of the system prior to any enhancement or optimization.

The results of the load flow demand and power loss estimation for the IEEE 14-bus power transmission network, incorporating both load and generation conditions, are presented comprehensively in Table 2. These results are

further visualized in Figure 3 and Figure 4. Together, they provide critical insights into the system's performance

under the given operating conditions.

Table 2: Line Flow Demand and Loss (Baseline Model)

From-To	Active Power Flow (MW)	Reactive Power Flow (MVAR)	Active Power Loss (MW)	Reactive Power Loss (MVAR)	Total Power Loss
1-2	89.742	40.016	187.112	571.280	601.141
1-5	229.100	90.083	3274.318	13516.636	13907.574
2-3	10.074	4.747	5.828	24.552	25.235
2-4	140.424	49.966	1290.938	3917.024	4124.270
2-5	139.358	50.067	1248.768	3812.745	4012.037
3-4	130.349	45.220	1275.588	3255.690	3496.661
4-5	-1.065	0.101	0.015	0.048	0.051
4-7	-0.280	0.110	0.000	0.019	0.019
4-9	-0.528	0.021	0.000	0.155	0.155
5-6	-119.075	-40.158	0.000	3979.778	3979.778
6-11	119.910	39.958	1517.321	3177.459	3521.152
6-12	119.579	39.976	1953.926	4066.664	4511.716
6-13	119.374	40.148	1049.279	2066.357	2317.502
7-8	-120.034	-30.182	0.000	2698.480	2698.480
7-9	-0.248	-0.089	0.000	0.008	0.008
9-10	0.527	0.076	0.009	0.024	0.026
9-14	0.147	0.216	0.009	0.018	0.020
10-11	-0.229	-0.196	0.007	0.017	0.019
12-13	-0.205	0.172	0.016	0.014	0.021
13-14	0.385	0.146	0.029	0.059	0.066

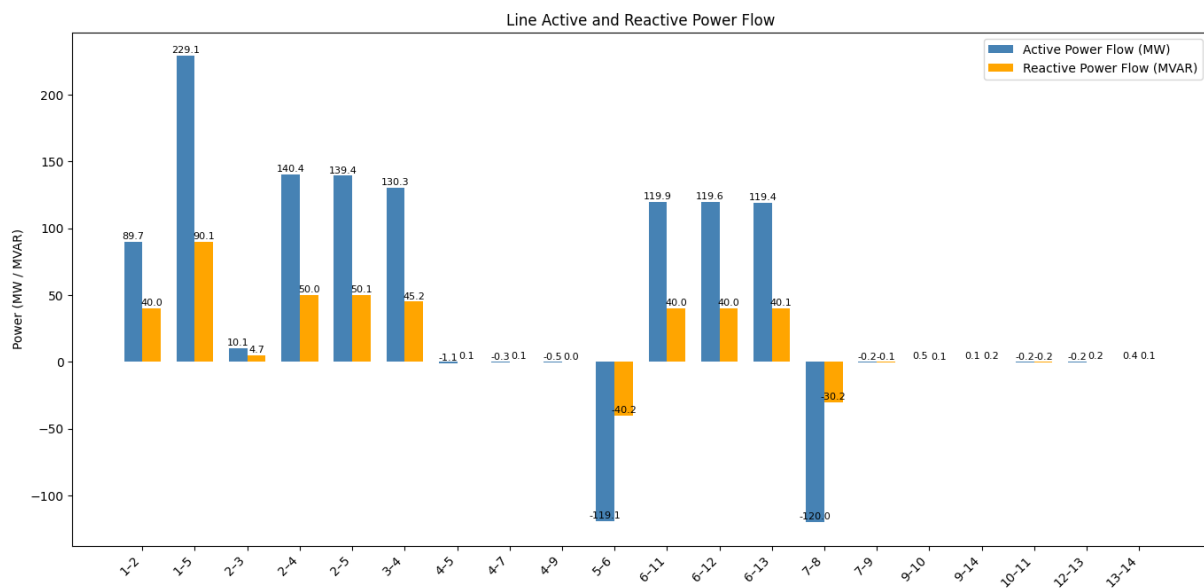


Figure 3: Active and reactive power demand

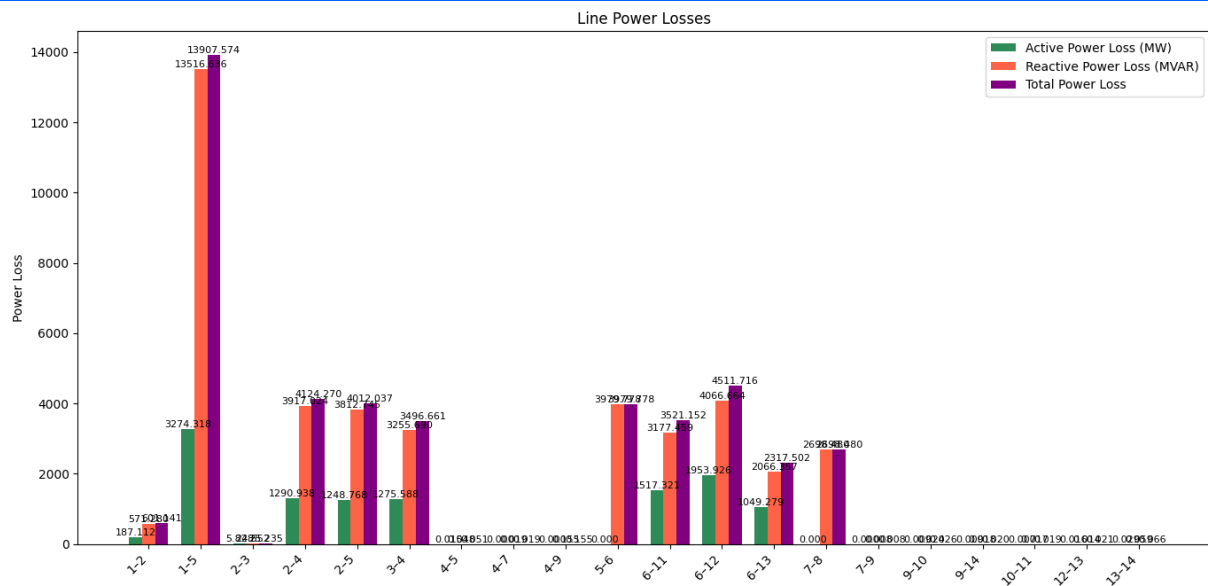


Figure 4: Line power losses

The active and reactive power flows across the various transmission lines, as seen in Table 2 and Figure 3, reveal the spatial distribution of power throughout the network. The highest active power transfer is observed along the line 1–5 (229.10 MW), which corresponds to one of the key transmission corridors linking the main generation centers with significant load areas. Similarly, the line 2–4 carries a substantial active load of 140.42 MW, indicating its strategic role in supporting the power transfer towards downstream buses. Conversely, some lines exhibit negative power flow values, such as 4–5 (–1.065 MW) and 7–8 (–120.034 MW). This negative sign is not an anomaly but a correct representation of the directionality of power transfer, indicating that power is effectively flowing in the reverse direction relative to the initial assumption. These directional reversals arise naturally in interconnected systems where distributed generation or varying load demands cause shifts in flow patterns. It also underscores the dynamic balance of supply and demand throughout the network. The reactive power flows mirror the trends in active power but exhibit notable variation in magnitude. This is expected, as reactive power management is heavily influenced by voltage regulation requirements, line reactance, and the presence of capacitive or inductive loads.

The corresponding line losses, presented alongside the flows in Table 2 and visualized in Figure 4, highlight the differential impact of power transfers on system efficiency. The lines 1–5, 2–4, 2–5, and 6–12 exhibit exceptionally high-power losses, with total losses reaching up to 13,907.57 units on line 1–5 alone. These large loss figures are attributed primarily to the higher current magnitudes resulting from substantial active and reactive power transfers combined with significant line impedance. A crucial observation is that lines with minimal or near-zero power transfer, such as 4–7, 4–9, 7–9, 9–14, correspondingly show negligible power losses. This reaffirms the principle that line losses scale approximately

with the square of the current, where current is minimal, losses remain small regardless of the physical length or impedance of the line. The presence of non-zero losses even on lines with negative power flows (e.g., 5–6, 7–8) further reinforces the correctness of the model. Losses are inherently non-directional in their calculation, being dependent on the absolute magnitude of current rather than the sign of the flow.

In the operation of power systems, the slack bus, also known as the swing or reference bus, plays a crucial role in maintaining the system's power balance and frequency stability. The slack bus compensates for real-time mismatches between total system generation and demand, and it absorbs any excess or deficit in both active and reactive power flow. In the IEEE 14-bus power transmission network considered for this study, Bus 1 serves as the designated slack bus, and its performance over time provides valuable insights into the dynamics of system-wide power variations.

The hourly active and reactive power injections of the slack bus over the entire simulation period, spanning a full year (8,760 hours) are presented in Figure 5. The results demonstrate clear temporal variability in both active power injection (measured in megawatts, MW) and reactive power injection (measured in megavolt-amperes reactive, MVAR), underscoring the dynamic nature of load demand and system response. The active power injection by the slack bus fluctuates significantly across the simulation horizon, with observed values ranging from approximately 15.59 MW at the lower end (e.g., 19:00 hours on December 31st) to peaks exceeding 85 MW (e.g., 01:00 hours on January 1st). This variation reflects the diurnal and seasonal changes in load demand patterns, as well as the contribution of other generation units within the system. Notably, the system experiences higher slack bus injections during peak demand periods, typically corresponding to evening hours when residential and commercial consumption tends to rise.

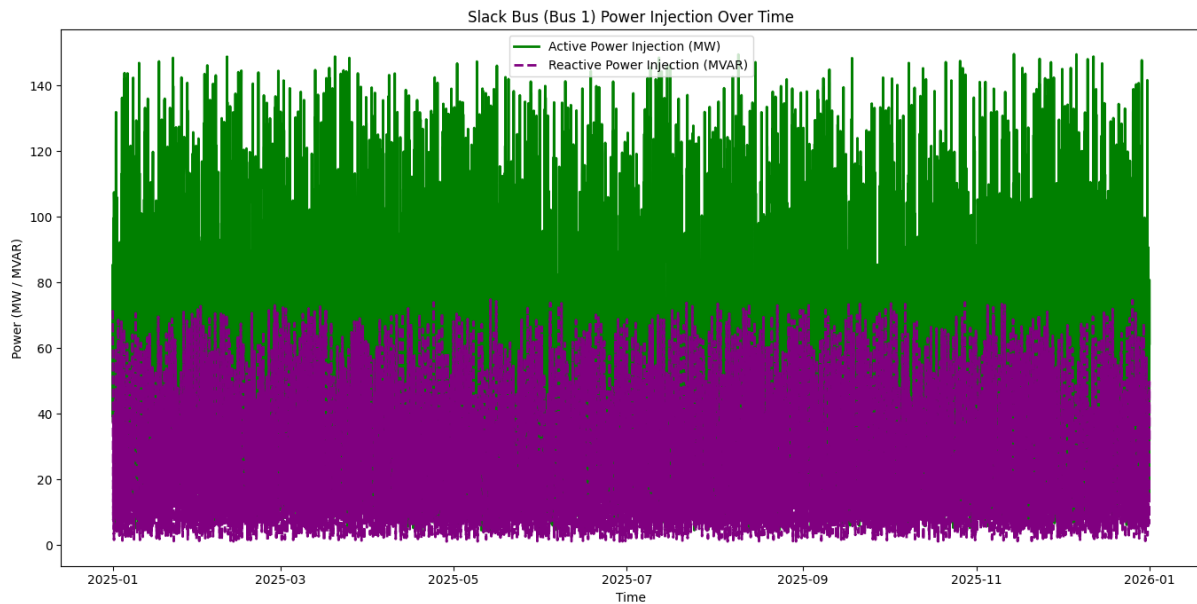


Figure 5: Slack bus power injection over time

Similarly, reactive power injection exhibits substantial variability, with values ranging from about 6.48 MVAR to nearly 71.55 MVAR over the year. The highest reactive power injections coincide with periods of heavy active power transfer, as the system compensates for increased reactive losses and maintains voltage stability. Conversely, during low-load periods, the reactive power requirements diminish, resulting in lower injections by the slack bus. One key observation is the presence of both high and moderate power injection phases, corresponding to distinct system loading conditions, such as weekdays with commercial activities versus weekends or holidays with reduced demand. These trends are essential for grid operators to monitor, as excessive reliance on the slack bus may indicate imbalances or inadequacies in distributed generation, load shedding, or voltage regulation. Figure 5 also illustrates these temporal variations graphically, allowing for easy identification of peak and off-peak

behaviours. The visualization also highlights the correlation between active and reactive power injections: while both follow similar trends, reactive power shows somewhat less pronounced peaks, which is consistent with the system's efforts to control voltage within permissible limits even when active power swings are significant.

The stability, efficiency, and reliability of an electrical power system are inherently linked to the voltage profile across the network and the amount of power loss incurred during transmission. Understanding how these two critical parameters evolve over time is essential for informed operational decision-making and long-term system planning. The results of this analysis, presented in Figure 6, offer valuable insights into the temporal trends of average bus voltage and total power losses within the IEEE 14-bus power transmission network over a full calendar year.

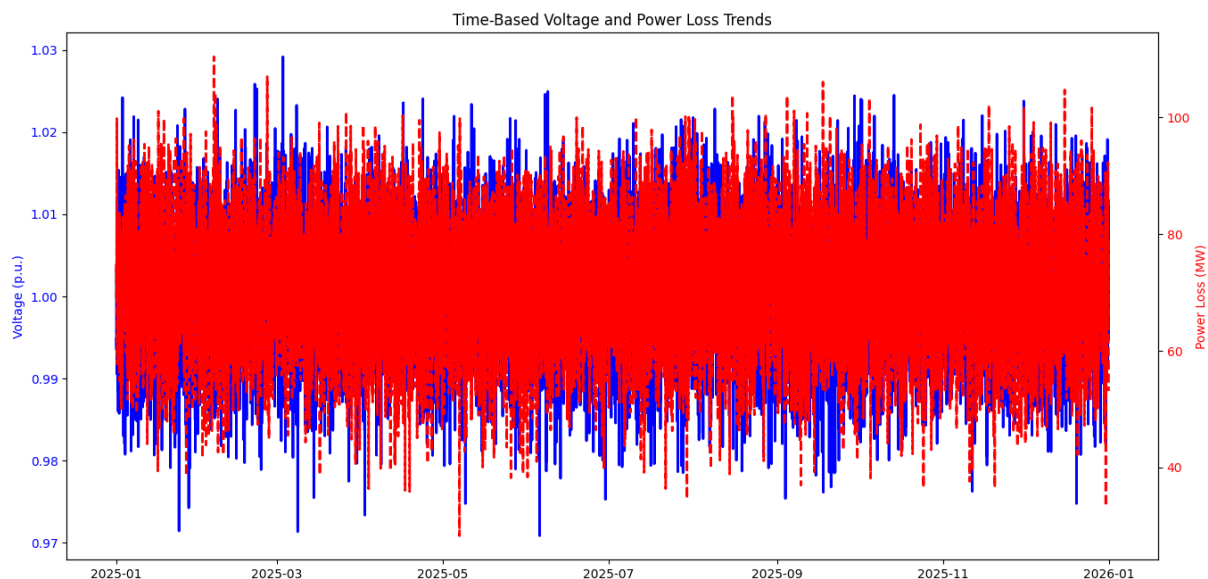


Figure 6: Time based voltage and power loss trends

The average voltage across all buses, measured in per unit (p.u.), exhibits a relatively stable behavior throughout the simulation period. The voltage values remain consistently close to the nominal value of 1.0 p.u., with slight oscillations observed in response to fluctuating system loads and generation patterns. Specifically, the average voltage ranges from approximately 0.9935 p.u. at the lower end to around 1.0118 p.u. at the upper bound. This stability reflects the effectiveness of the voltage control mechanisms embedded within the network, particularly the presence of generator buses (PV buses) and the slack bus that actively regulate voltage levels. The minor deviations from the nominal voltage are typical in practical power systems and can often be attributed to variations in load demand, line impedances, reactive power flows, and the operational status of shunt capacitors or transformer tap changers. Periods of voltage dip, such as the instance recorded at 01:00 hours on January 1st (0.9935 p.u.), are likely correlated with peak load conditions where reactive power support becomes strained. Conversely, slight voltage elevations above 1.01 p.u. are often observed during off-peak hours when the system is lightly loaded, resulting in less voltage drop across transmission lines. Maintaining voltages within acceptable bounds is vital for protecting sensitive equipment, minimizing transmission losses, and ensuring overall system security. The trends observed in Figure 4.6 indicate that the system operates within a well-regulated voltage envelope, although continuous monitoring is essential to detect and mitigate potential voltage instability risks.

In tandem with voltage variations, the total active power loss across the network shows a distinct temporal

pattern, heavily influenced by the dynamic nature of system demand. The total power losses fluctuate between approximately 53.12 MW and 83.61 MW over the course of the year. The highest losses, such as the 83.61 MW recorded at 03:00 hours on January 1st, align with periods of elevated power transfer, which inherently increases current flow and, by extension, I²R losses in the transmission lines. Conversely, the lowest losses, such as the 53.12 MW observed at 23:00 hours on December 31st, occur during periods of reduced load, when less power is being transferred and line currents are minimized. This inverse relationship between system loading and power losses is consistent with fundamental power system principles. The nature of the power loss curve, as depicted in Figure 6, highlights the need for demand-side management, distributed generation integration, and network reconfiguration strategies to reduce losses and improve overall system efficiency. Furthermore, high loss periods may indicate congestion or bottlenecks within specific transmission corridors, warranting potential network reinforcement or optimization interventions.

The voltage stability of a power system is a critical aspect of its operational integrity, reflecting the system's ability to maintain acceptable voltage levels under varying load conditions and disturbances. The Voltage Stability Index (VSI), presented in Figure 7, provides a quantitative measure of proximity to voltage instability or collapse. Typically, values closer to 1 indicate robust voltage stability, while values significantly lower than 1 suggest heightened vulnerability.

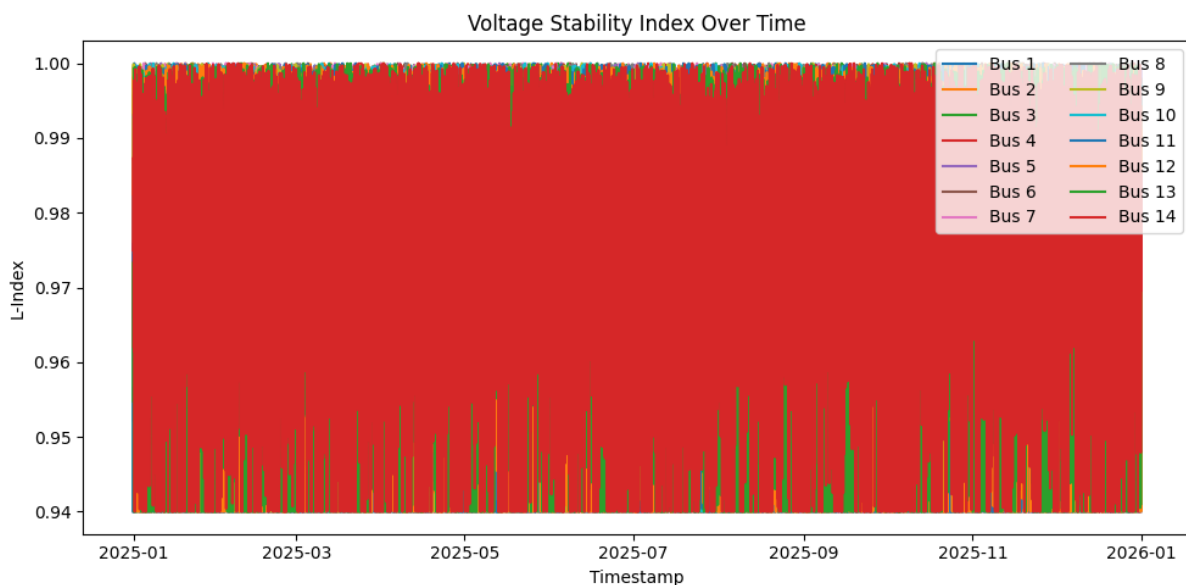


Figure 7: Stability index plot

The results obtained from the year-long simulation reveal that the VSI for the IEEE 14-bus power transmission network remains consistently high throughout the period, with values ranging approximately from 0.9697 to 0.9783.

This narrow band of variation demonstrates that the system is operating well within stable voltage limits across all timestamps evaluated.

The per bus voltage profile statistics for IEEE 14-Bus are presented in Table 3 and Figure 8. The voltage profile analysis conducted across all buses in the IEEE 14-bus distribution network reveals that the voltage magnitudes remained within the acceptable regulatory bounds of 0.94 to 1.06 per unit, as recommended by IEEE Std 1159 and related operational norms. This compliance across all 14 buses is a critical indicator of proper reactive power balance, controlled network loading, and sufficient voltage support mechanisms within the modeled network. From Table 2, it is evident that the minimum and maximum voltage values are identical for all buses, each ranging from 0.94 pu to 1.06 pu, suggesting that the network simulation includes both high-load (peak) and low-load (off-peak) scenarios. These extremities correspond to the outer bounds of expected daily operational voltages and likely reflect worst-case voltage drops and rises, respectively. The average voltage magnitude across all buses fluctuates only within the narrow band of 0.9993 to 1.0008 pu, indicating

an extremely well-balanced system under baseline (unoptimized) conditions. This high degree of voltage consistency suggests that, at this stage, no bus is subject to chronic under- or over-voltage conditions, which is a desirable property in both operational and planning contexts.

More specifically, bus 3 records the highest average voltage magnitude of 1.000837 pu, which could imply it benefits from close proximity to a strong voltage support source (such as a generator or regulated transformer). Conversely, Bus 6 has the lowest average voltage magnitude of 0.999376 pu, which still comfortably falls within nominal tolerance and may be attributed to its network depth or cumulative impedance. Buses such as 1, 5, 7, 10, 14 all maintain average values tightly clustered around 1.0004 pu, further reinforcing uniform voltage performance across the network.

Table 3: Per-Bus Voltage Profile Statistics for IEEE 14-Bus power transmission network

Bus ID	Min Voltage (pu)	Max Voltage (pu)	Avg Voltage (pu)
1	0.94	1.06	1.000197
2	0.94	1.06	1.000031
3	0.94	1.06	1.000837
4	0.94	1.06	0.999759
5	0.94	1.06	1.000349
6	0.94	1.06	0.999376
7	0.94	1.06	1.000433
8	0.94	1.06	1.000470
9	0.94	1.06	0.999509
10	0.94	1.06	1.000478
11	0.94	1.06	1.000342
12	0.94	1.06	1.000211
13	0.94	1.06	1.000224
14	0.94	1.06	1.000435

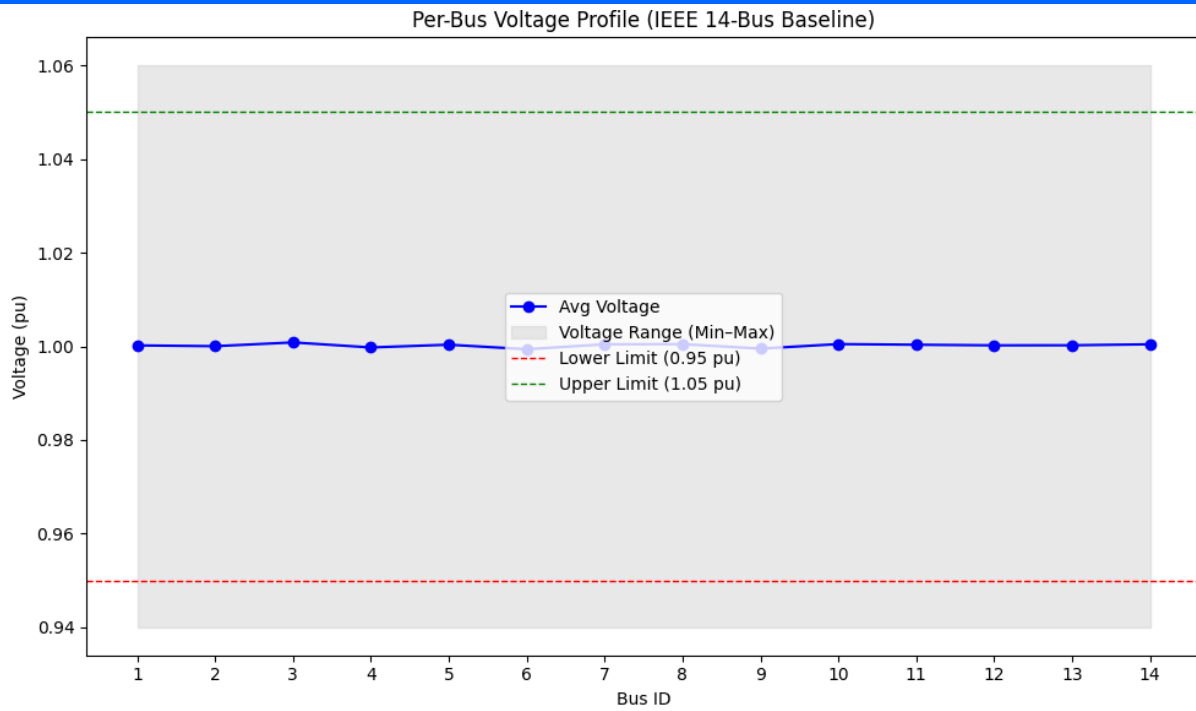


Figure 8: Per-Bus Voltage Profile Statistics for IEEE 14-Bus power transmission network

Additionally, the result confirms that the modelled system is inherently voltage stable, requiring minimal post-processing correction at the baseline level. Future improvements will therefore aim at optimizing transient voltage behaviours, reactive support efficiency, and resilience to contingencies, rather than correcting fundamental voltage violations.

A fundamental requirement for the stable and reliable operation of any electric power system is the ability to maintain an exact or near-exact balance between power

generation and power consumption across all buses in the network.

The computed active ($P_{mismatch}$) and reactive ($Q_{mismatch}$) power mismatches for each bus in the IEEE 14-bus power transmission network are present in Table 4 and Figure 9. The mismatch values were obtained by comparing the average power demand at each bus, extracted from the simulated dataset, against the assigned generation capacities based on the standard classification of bus types. In this system, five buses (Bus 1, Bus 2, Bus 3, Bus 6, and Bus 8) were designated as generator buses, with Bus 1 serving as the slack or swing bus. The remaining buses were treated as pure load buses with no embedded generation.

Table 4: Per-Bus Active and Reactive Power Mismatch Summary

Bus ID	$P_{mismatch}$ (MW)	$Q_{mismatch}$ (MVAR)
1	173.824	65.994
2	84.083	25.978
3	74.008	21.231
4	-56.341	-23.988
5	-55.276	-24.089
6	63.799	16.069
7	-56.061	-24.098
8	63.973	6.084
9	-55.813	-24.009
10	-56.340	-24.085
11	-56.111	-23.888
12	-55.780	-23.906
13	-55.575	-24.078
14	-55.960	-24.224

The ability of a power system to maintain an exact balance between scheduled power injections and calculated power flows is a fundamental indicator of network solvability and physical realism in load flow analysis. Table 4, visualized in Figure 9 summarizes the active (P) and reactive (Q) power mismatches for each bus across the IEEE 14-bus power transmission network. These values reflect the numerical deviation between scheduled and computed power flows, as determined using nonlinear power flow equations.

As seen in Table 3, the generator buses which include Bus 1, Bus 2, Bus 3, Bus 6, and Bus 8, recorded positive active and reactive power mismatches. This is a desirable and expected outcome, as these buses supply more power than they consume locally. The surplus power at these generator buses is what enables the network to meet the demands of

non-generator buses and to compensate for losses that naturally occur along transmission lines. Bus 1 (Slack Bus) showed the highest positive mismatch, with an active power surplus of 173.824 MW and a reactive power surplus of 65.994 MVAR. This reflects its role as the balancing bus, absorbing any system-wide imbalance and maintaining system voltage and frequency stability. Bus 2 and Bus 3 (PV buses) also contributed significant active power surpluses of 84.083 MW and 74.008 MW respectively, alongside notable reactive power contributions. These values emphasize their role in voltage control and load sharing. Bus 6 and Bus 8, while operating as PV buses, exhibited smaller surpluses (63.799 MW and 63.973 MW respectively), yet their contributions are vital in supporting the overall power flow equilibrium.

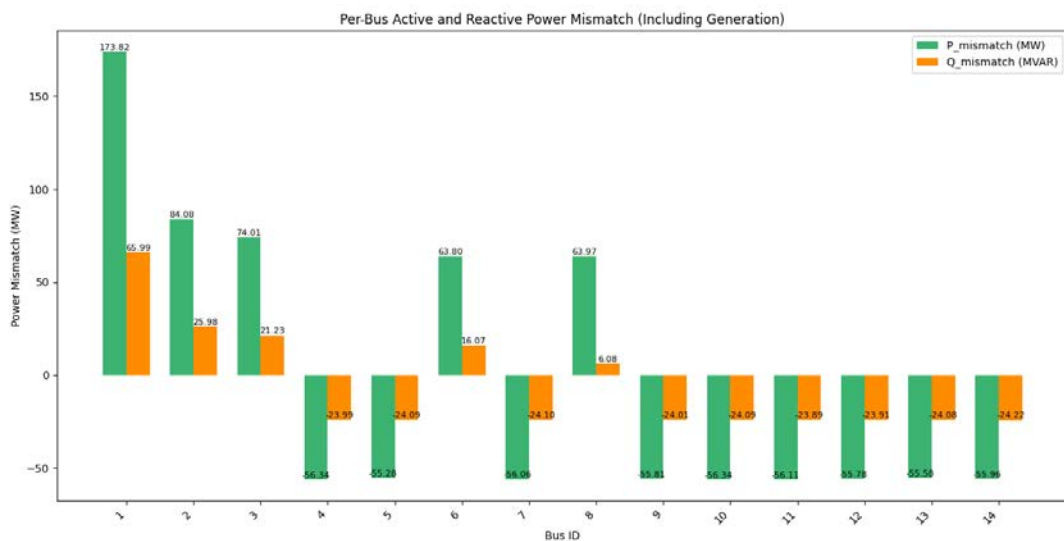


Figure 9: Per-Bus Active and Reactive Power Mismatch (Baseline Load Flow Analysis)

In contrast, all the load-only buses (PQ buses) which include: buses 4, 5, 7, 9, 10, 11, 12, 13, and 14, exhibited negative mismatches in both active and reactive power. This indicates that these buses consume more power than they generate (in this case, they have no generation at all), resulting in net deficits that must be supplied from elsewhere in the network. The negative mismatches are relatively uniform across these buses, with active power deficits clustering around -55 to -56 MW and reactive power deficits ranging between -23.8 MVAR and -24.2 MVAR. This uniformity is indicative of the homogenous distribution of loads within the system as captured by the synthetic dataset used in the simulation. The marginal differences in mismatch values can be attributed to slight variations in the specific load demand profiles at each bus, which are inherently time-varying in a real system but averaged here for baseline assessment. The graphical representation in Figure 9 vividly illustrates the mismatch pattern across the 14-bus power transmission network. The positive bars highlight generator buses that serve as power sources, while the negative bars depict load buses that represent power sinks.

4. Conclusion

In this study, a comprehensive load flow analysis was conducted on the IEEE 14-bus power transmission network using simulated bus-level demand data alongside the transmission line parameters characterizing the network. The objective was to evaluate both the power demand distribution and the line power losses across the network. Also, voltage profiles, loss distributions, slack bus behaviour, and stability indices were each captured for selected timestamps (e.g., peak and off-peak periods), providing insights into the natural operating performance of the system prior to any enhancement or optimization. The voltage profile analysis conducted across all buses in the IEEE 14-bus distribution network reveals that the voltage magnitudes remained within the acceptable regulatory bounds of 0.94 to 1.06 per unit, as recommended by IEEE Std 1159 and related operational norms. This compliance across all 14 buses is a critical indicator of proper reactive power balance, controlled network loading, and sufficient voltage support mechanisms within the modeled network.

References

1. Khan, A., Khan, M. S., & Wang, Y. (2025). Enhancing Energy Efficiency in Power Systems: Particle Swarm Optimization for Minimizing Power Losses in the IEEE 14-Bus System: Enhancing Energy Efficiency in Power Systems: Particle Swarm Optimization for Minimizing Power Losses in the IEEE 14-Bus System. *International Journal of Electrical Engineering and Applied Sciences (IJEAS)*, 8(1).
2. Thota, P. K., Somaskandan, G., & Mani, M. (2023). The Voltage stability analysis for grid-connected PV system using optimized control tested by IEEE 14 & 30 bus system. *Int. J. Exp. Res. Rev*, 30, 109-118.
3. Peyghami, S., Davari, P., Fotuhi-Firuzabad, M., & Blaabjerg, F. (2019). Standard test systems for modern power system analysis: An overview. *IEEE industrial electronics magazine*, 13(4), 86-105.
4. Ibrahim, I. A., & Hossain, M. J. (2021). Low voltage distribution networks modeling and unbalanced (optimal) power flow: A comprehensive review. *IEEE Access*, 9, 143026-143084.
5. Hassan, M. H., Kamel, S., Alateeq, A., Alassaf, A., & Alsaleh, I. (2023). Optimal power flow analysis with renewable energy resource uncertainty: a hybrid AEO-CGO approach. *IEEE Access*, 11, 122926-122961.
6. Hayes, B., Hernando-Gil, I., Collin, A., Harrison, G., & Djokić, S. (2014). Optimal power flow for maximizing network benefits from demand-side management. *IEEE transactions on power systems*, 29(4), 1739-1747.
7. Jereminov, M., Hooi, B., Pandey, A., Song, H. A., Faloutsos, C., & Pileggi, L. (2019, August). Impact of load models on power flow optimization. In *2019 IEEE Power & Energy Society General Meeting (PESGM)* (pp. 1-5). IEEE.
8. Risi, B. G., Riganti-Fulginei, F., & Laudani, A. (2022). Modern techniques for the optimal power flow problem: State of the art. *Energies*, 15(17), 6387.
9. Ntombela, M., Musasa, K., & Leoaneka, M. C. (2022). Power loss minimization and voltage profile improvement by system reconfiguration, DG sizing, and placement. *Computation*, 10(10), 180.
10. Mahato, J. P., Poudel, Y. K., Mandal, R. K., & Chapagain, M. R. (2024). Power loss minimization and voltage profile improvement of radial distribution network through the installation of capacitor and distributed generation (DG). *Archives of Advanced Engineering Science*, 1-9.
11. Essallah, S., & Khedher, A. (2020). Optimization of distribution system operation by network reconfiguration and DG integration using MPSO algorithm. *Renewable Energy Focus*, 34, 37-46.
12. Von Meier, A. (2024). *Electric power systems: a conceptual introduction*. John Wiley & Sons.
13. Ten, C. W., & Hou, Y. (2024). *Modern power system analysis*. CRC Press.
14. Kumar, A., Jha, B. K., Das, S., & Mallipeddi, R. (2021). Power flow analysis of islanded microgrids: A differential evolution approach. *IEEE Access*, 9, 61721-61738.
15. Raza, A., Zahid, T., Iqbal, S., Ahmad, I., & Hussain, J. (2024). Optimizing Power Flow: A Study of Newton Raphson (NR) Method for Load Flow Analysis (LFA) in Power Systems. *Innovative Computing Review*, 4(1), 37-50.
16. Nouredine, T., & Djamel, L. (2021). Load flow analysis using Newton-Raphson method in presence of distributed generation. *International journal of power electronics and drive systems*, 12(1), 489.
17. Mohsin, M. Y., Khan, M. A. M., Yousif, M., Chaudhary, S. T., Farid, G., & Tahir, W. (2022). Comparison of Newton Raphson and Gauss Seidal Methods for Load Flow Analysis. *International Journal of Electrical Engineering & Emerging Technology*, 5(1), 01-07.
18. Nwachukwu, S. E. (2025). Power Flow Analysis of a 5-Bus Power System Based on Newton-Raphson Method. *arXiv preprint arXiv:2506.23425*.
19. Awal¹, L. J., Syahbani, M. A., & Abdillah, W. (2024, November). System Based On the Value Of Voltage Sag And Phase Angle Using Matching Approach. In *Proceedings of the International Conference on Advanced Technology and Multidiscipline (ICATAM 2024)* (Vol. 245, p. 178). Springer Nature.
20. Mander, D. K., & Viridi, G. S. (2017). Result analysis on load flow by using Newton Raphson method. *International Journal of Advanced Research in Electrical, Electronics and Instrumentation Engineering*, 6(7), 5835-5844.